Performance modelling of a partially-aerated submerged fixed-film bioreactor:

Kordkandi, Salman Alizadeh; Khosfetrat, Ali Baradar; Faramarzi, Asaad

DOI:
10.1016/j.jiec.2017.12.039

Document Version
Peer reviewed version

Citation for published version (Harvard):
Kordkandi, SA, Khosfetrat, AB & Faramarzi, A 2017, 'Performance modelling of a partially-aerated submerged fixed-film bioreactor: Mechanistic analysis versus semi data-driven method', *Journal of Industrial and Engineering Chemistry*. https://doi.org/10.1016/j.jiec.2017.12.039

Title: Performance modelling of a partially-aerated submerged fixed-film bioreactor: Mechanistic analysis versus semi data-driven method

Authors: Salman Alizadeh Kordkandi, Ali Baradar Khoshfetrat, Asaad Faramarzi

PII: S1226-086X(17)30701-3
DOI: https://doi.org/10.1016/j.jiec.2017.12.039
Reference: JIEC 3795

To appear in:

Received date: 25-7-2017
Revised date: 17-12-2017
Accepted date: 19-12-2017

Please cite this article as: Salman Alizadeh Kordkandi, Ali Baradar Khoshfetrat, Asaad Faramarzi, Performance modelling of a partially-aerated submerged fixed-film bioreactor: Mechanistic analysis versus semi data-driven method, Journal of Industrial and Engineering Chemistry https://doi.org/10.1016/j.jiec.2017.12.039

Performance modelling of a partially-aerated submerged fixed-film bioreactor: Mechanistic analysis versus semi data-driven method

Salman Alizadeh Kordkandi[a,b], Ali Baradar Khoshfetrat[a,b]*, Asaad Faramarzi[c]

[a] Chemical Engineering Faculty, Sahand University of Technology, Tabriz, 51335-1996 Iran

[b] Environmental Engineering Research Center (EERC), Sahand University of Technology, Tabriz, 51335-1996 Iran

[c] School of Civil Engineering, University of Birmingham, Edgbaston, Birmingham, B15 2TT, United Kingdom

* Corresponding author: Ali Baradar Khoshfetrat

E-mail: khoshfetrat@sut.ac.ir

Tel: +98-411-345-9162

Fax: +98-411-344-4355

Graphical abstract

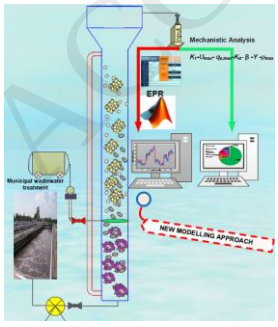

Highlights

- Mechanistic and semi-data driven methods were used to model a partially-aerated ASFF.
- Among mechanistic models, Stover-Kincannon could fairly predict COD removal.
- Evolutionary computing EPR developed an accurate explicit model for COD removal.
- EPR model showed a promising alternative to model biofilm bioreactor systems.

Abstract

A novel semi-mechanistic data-driven technique based on an evolutionary polynomial regression (EPR) was developed along with a kinetic analysis to evaluate the performance of an external loop upflow partially-aerated fixed-film bioreactor (UP/ASFF). Modelling of experimental data was carried out under different organic loading rates (OLR), solid retention time (SRT), and food to microorganisms' ratio (F/M ratio). The results showed that the EPR model was the best approach for the performance evaluation of the UP/ASFF system with R^2 of 0.93 and normalized MSE of 0.02 although the Stover-Kincannon's model showed also a promising predication with high accuracy and R^2 of 0.92.

Keywords*:* Process analysis; Kinetics modelling; Evolutionary polynomial regression; upflow partially-aerated fixed-film bioreactor.

Nomenclatures:

Abbreviation	Description	Abbreviation	Description
V	Reactor volume (L)	S_e	Effluent COD concentrations (mg/L)
Q	Inflow rate (L/d)	K_s	Half saturation concentration (mg/L)

K_2	Grau second-order kinetic constant (1/d)	K_1	First-order kinetic constant (1/d)
K_d	Microbial death rate constant (1/d)	K_B	Saturation value constant (kg/(m^3.d))
X	Biomass concentration at the reactor (mgVSS/L)	μ	Specific growth rate (1/d)
X_e	Effluent biomass concentration (mgVSS/L)	β	Kinetic parameter for the Contois model (mgCOD/(mgVSS))
X_i	Influent biomass concentration (mgVSS/L)	SRT	Solid retention time (d)
Y	Yield coefficient (mgVSS/mgCOD)	S_i	Influent COD concentrations (mg/L)
S	COD concentrations in the bioreactor (mg/L)	HRT	Hydraulic retention time (d)
U_{max}	Maximum utilization rate constant (kg/(m^3.d))	μ_{max}	Maximum specific growth rate (1/d)
F/M	Food to microorganism ratio (kgCOD/(kgVS.d))	E	COD removal efficiency (%)
$q_{s,max}$	Contois maximum specific substrate utilization rate	CD	Coefficient of Determination

1. Introduction

Over the last couple of decades, more consideration has been given to the potential methodology for wastewater treatment [1,2,3,4,5,6]. These processes are efficient, in particular, for in industrial water and wastewaters treatment [7,8,9,10,11,12]. While there are several non-selective physiochemical methodologies in terms of contaminants removal with such features [13,14,15,16,17], application of efficient microbial community for waste management can be considered as a robust alternative [18,19,20,21]. Biological processes are recommended to treat municipal wastewater due to their potentials for simultaneous removals of inorganic nitrogen and carbon, as well as energy and cost savings. Modern biological wastewater treatment plants usually consist of interconnected units such as aerobic, anoxic, anaerobic, and physicochemical processes to achieve higher performance efficiencies. Upflow partially-aerated fixed-film bioreactor (UP/ASFF) system, which provides both aerated and non-aerated zones

inside a single bioreactor, can simultaneously remove nutrients and carbonaceous matters of municipal wastewaters. Although performance evaluation of the UP/ASFF bioreactor system for municipal wastewater treatment has been carried out by some researchers [22,23,24], its performance modelling and analysis have not been reported yet.

Generally, finding a solution for governing equations that comprise the reaction, mass transfer, bioreactor hydrodynamics, biofilm dynamics, and shear stress [22] is a major challenge for studying the performance of biofilm bioreactors. Particularly, where the bioreactor comprises of two semi-anaerobic and aerobic zones (diverse in microbial types and the associated performance) without physical separation. Therefore, modelling this system can be a useful approach to attain several outcomes such as interpreting the performance of the system, analyzing its behavior, and estimating the responses under various conditions [25].

Almost application of modelling in various fields of wastewater treatment in different scales has been progressed [1,5,9,10,26,27]. A knowledge-based model aims at describing the performance of a process via certain fundamental laws (i.e. continuity equations) and expressing mechanistic relationships between dependent and independent variables [26]. Moreover, several experiments will be required to determine the influence of environmental factors, such as hydraulic loading, substrate loading, toxic substances, and temperature [23]. Kinetic analysis is one of the best known means of describing the behaviors of biological wastewater treatment systems [28] which simplifies the assessment of pollutant degradation rate. Furthermore, the determined kinetic parameters can be used for the design, operation and optimization of bioreactors such as UP/ASFF [29]. In this context, some models such as first-order,

second-order, Stover-Kincannon, Monod, and Contois are used competently to describe dominant processes [30,31,32,33].

On the other hand, data-based modelling techniques can be expensive due to the requirement of a large amounts of data from the process for building and validation of the model. Empirical models do not require a priori knowledge on the mechanistic of system. Between the empirical modelling and mechanistic modelling, there is a hybrid modelling in which some physical insights are available, but several parameters will be remained for determining the observed data [34]. Hybrid modelling leads to better models of the process, which are more transparent or physically interpretable and have better generalization properties than empirical models [35]. Evolutionary Polynomial Regression (EPR) is a hybrid modelling approach integrating machine learning based algorithms with symbolic regression and has proven to be a robust, promising approach to simulate complex physical, and chemical phenomena [36,37]. The design and operation of complex plants is a challenging issue that could be easily tackled by the EPR modelling approach.

In our pervious study, the performance of the UP/ASFF bioreactor system without physical separation was assessed in terms of energy and cost savings prospects as well as the removal efficiencies of nitrogen and carbon from synthetic and real municipal wastewaters [23].

The main aim of this study was to introduce a promising alternative modelling technique for the conventional kinetic analysis in the area of biofilm process. Up to now, most modelling approaches of biofilm processes have been developed based on the kinetic perspective, which is a conventional strategy, and in some cases, these approaches suffer from several drawbacks including representing a low coefficient of determination between predicted values and the experimental data. To address this

drawback and develop a more comprehensive insight into the physical phenomenon of biofilm process, the EPR approach was used. Accordingly, at first step, all the current kinetic models were thoroughly evaluated. The associated drawbacks and inefficiencies of each kinetic model were determined. Then to overcome the identified problems, the EPR modelling approach was introduced as a grey box modelling strategy.

2. Materials and methods

2.1. Experimental set-up and operation

The UP/ASFF bioreactor was a cylindrical Plexiglas with 5 mm thickness and inside diameter of 11 cm. The effective working volume of the bioreactor was 7.6 L. In order to provide a support for biomass attachment and growth, the bioreactor was filled with polypropylene media with an estimated available surface area of 320 $m^2.m^{-3}$ (porosity of 0.89).

Semi-anaerobic (non-aerated) and aerobic (aerated) parts within the bioreactor were formed by introducing air to the middle point of the column which has been filled by polypropylene media. To provide an upflow wastewater current, first, influent wastewater was introduced into the bottom of the bioreactor (semi-anaerobic zone), and then it passed through an aerobic zone, while the zones were connected by a 15 mm diameter recycle loop. Three ports were embedded along the bioreactor for sampling purposes. In addition, a perforated plate was installed at the top of the packed media to keep them submerged in the bioreactor. To initiate the experiment, the bioreactor was filled with 1 L seeding sludge at an average room temperature (25±3 ^{0}C).

2.2. Analytical methods and wastewater

Synthetic wastewater was prepared by adding sodium acetate, ammonium chloride, and potassium dihydrogen phosphate as carbon, nitrogen, and phosphor source into the tap

water, as described by Borghei et al. [38] . The influent COD concentrations varied from 200 to 1200 $mg.L^{-1}$. All the chemicals used in the experiments were analytical grade.

Samples of effluent were centrifuged before the analysis. Soluble COD at the influent and effluent samples were determined by closed reflux colorimetric method [39]. The total suspended solids (TSS) and volatile suspended solids (VSS) of samples were measured by weighting after drying and burning at 103–105 °C, and 550 °C, respectively [39]. The dissolved oxygen (DO) concentration was measured with a DO meter (Cyberscan DO 300, Eutech Instruments Pte Ltd). Temperature and pH were measured with the same electrode (HANNA instrument HI 8314).

3. Model development

Mathematical models can be introduced in many forms, from simple realistic correlations to sophisticated and computationally intensive processes. In the present study, mechanistic approaches were developed based on first-order, second-order, modified Stover-Kincannon, Monod, and Contois models. Besides mechanistic models, a semi-mechanistic approach (EPR) was used to develop mathematical structures, which derived through conceptualization of physical phenomena or through simplification of differential equations describing the phenomena under consideration. An analysis of variance test was performed to determine the statistical significant differences between the experimental data and the predicted values by models. Furthermore, some criteria such as F-test, P-value, normalized MSE, and R^2 were considered for this purpose.

3.1. Mechanistic modelling

3.1.1. First-order kinetic model

A mass balance equation for the COD removal in the bioreactor is given by Eq. (1), where Q, V, S_i, S_e, and K_1 are inflow rate, bioreactor volume, influent COD, effluent COD, and first-order kinetic constant, respectively. Under a steady state condition, the COD accumulation (-dS/dt) is negligible, and Eq. (1) can be reduced to the Eq. (2), where HRT is hydraulic retention time (V/Q). First-order reaction kinetics show the plotting of eliminated OLR versus effluent concentration, which gives straight line for determining K_1 (first-order substrate removal rate constant).

$$-dS/dt = (QS_i/V) - (QS_e/V) - K_1 S_e \quad (1)$$

$$S_i - S_e / \mathrm{HRT} = K_1 S_e \quad (2)$$

3.1.2. Grau second-order kinetic model

Studies demonstrated that the second-order model was more applicable than first-order in biofilm reactor [33,38]. In addition, the Grau second-order model was appropriate for predicting nitrogen removal [40]. The general equation for the Grau second-order kinetic model can be expressed as Eq. (3) [41]. If Eq. (3) was integrated and then linearized, Eq. (4) will be obtained. Knowing that organic matter removal efficiency is equal ((S_i-S_e)/S_i) and expressed as E, Eq. (4) can be rewritten in the form of Eq. (5).

$$-dS/dt = K_2 X (S_e/S_i)^2 \quad (3)$$

$$S_i.\mathrm{HRT}/S_i - S_e = \mathrm{HRT} + S_i/XK_2 \quad (4)$$

$$\mathrm{HRT}/E = n\mathrm{HRT} + m \quad (5)$$

where m equals to $S_i/(K_2X)$, and n in Eq. (5) is close to one. K_2 is the rate constant of Grau second-order substrate removal (1/d) and X is the biomass concentration in the bioreactor (gVSS/L). The kinetic constant values, m and n can be obtained from the Eq. (5) by plotting a graph of HRT/E versus HRT.

3.1.3. Modified Stover–Kincannon model

Kincannon and Stover developed a mathematical model based on a relationship between the specific substrate utilization rate and total organic loading [42]. For the first time, this model was used for rotating biological contactor, which shows that it was appropriate for kinetic analysis of a complicated anaerobic and aerobic processes [42]. The widespread application of this model is due to its simplicity and the modelling ignoring parameters, such as substrate diffusion and hydraulic dynamics, which may be important to the bioreactor performance [43]. The following Eqs. (6-8) describe the modified Stover–Kincannon model. dS/dt is the substrate removal rate (kg /(m^3.d)) and is defined as Eq. (7). Accordingly, by considering Eq. (6) and (7), Eq. (8) can be obtained and illustrated as follows:

$$dS/dt = U_{max} \cdot (Q \cdot S_i / V) / K_B + (Q \cdot S_i / V) \quad (6)$$

$$dS/dt = Q/(V \cdot (S_i - S_e)) \quad (7)$$

$$V/Q \cdot (S_i - S_e) = (K_B . V / U_{max} . Q \cdot S_i) + 1/U_{max} \quad (8)$$

3.1.4. Monod and Contois models

Monod kinetics model is used extensively to study biomass growth/decay rate and expressed as Eqs. (9-10). The ratio of the total biomass in the bioreactor to the wasted

biomass per given time represent solid resistant time (SRT) and it can be calculated from Eq. (11). It should be noted that SRT is calculated based on the VSS and the attached biomass on support. In spite of a fair similarity of Contois and Monod models in terms of the type of equation, the Monod relation only depends on concentration of the substrate [44]. In addition, the Contois growth model is able to describe the aerobic degradation of wastewater treatment.

$$dX / dt = QX_i / V - QX_e / V + \mu X - XK_d \quad (9)$$

$$-dS / dt = QS_i / V - QS_e / V - \mu X / Y \quad (10)$$

$$\mathrm{SRT} = XV / QX_e \quad (11)$$

$$\mu = \mu_{max} . S_e / K_s + S_e \quad (12)$$

$$\mu = \mu_{max} . S_e / \beta X + S_e \quad (13)$$

Monod and Contois models in accordance with Eqs. (12) and (13) can express the relationship between μ and S_e. Under a steady state condition, while the concentration of biomass in the influent flow is considered zero, the following equations can be obtained by substituting and rearranging Eqs. (11-13) into Eqs. (9-10). Then plotting $((S_i-S_e)/\mathrm{HRT}.X)$ versus (1/SRT) in Eq. (16), the values for coefficients Y and K_d will be determined.

$$\mu = (1/\mathrm{SRT}) + K_d \quad (14)$$

$$\mu_{max} . S_e / (K_s + S_e) = (1/\mathrm{SRT}) + K_d \quad (15)$$

$$(S_i - S_e) / (\mathrm{HRT}.X) = (1/Y).(1/\mathrm{SRT}) + (1/Y).K_d \quad (16)$$

also, the values of μ_{max} and K_s can be determined by plotting Eq. (17), which is derived from Eq. (15):

$$\mathrm{SRT}/1 + (\mathrm{SRT}.K_d) = (K_s / \mu_{max}).(1/S_e) + 1/\mu_{max} \quad (17)$$

by substituting Eq. (13) instead of the Monod equation into Eq. (9), Eq. (19) can be derived from rearranging Eq. (18).

$$\mu_{max}.S_e / (\beta X + S_e) = (1/SRT) + K_d \quad (18)$$

$$SRT/(1+SRT.K_d) = (\beta.X) / (\mu_{max}.S_e) + (1/\mu_{max}) \quad (19)$$

According to Eq. (19), if the quotient (SRT)/ (1+SRT.K_d) was plotted against the quotient X/S_e, μ_{max} could be calculated by intercept determination of the straight line, and subsequently β can be obtained from the slope determination.

3.2. Hybrid modelling

Evolutionary polynomial regression is a hybrid data-driven method for creating pseudo-polynomial models based on evolutionary computing [35]. In general, EPR follows a two-stage procedure for constructing symbolic models [34,36,45]. At first, a mathematical structure of models is developed by exploiting a special coding of expressions, which permits the use of a heuristic search by using a multi-objective genetic algorithm named OPTIMOGA [46]. Then, it performs a numerical regression to find the parameters of the model (i.e. coefficients of pseudo-polynomial terms) [36]. A general EPR expression may be given as Eq. (20).

$$G = \sum_{j=1}^{p} a_j \varphi\left(x, f(x)\right) + a_0 \quad (20)$$

where G is the model output; a_j is a constant value; φ is a function constructed by the process; x is the matrix of input variables; f is a function selectable by the user and p is the maximum length (number of terms) of the polynomial expression (bias a_0 excluded).

Based on the general symbolic expressions in Eq. (20), the EPR involves several classes of mathematical expressions which may include functions definable by the user (see [36,47]).

In this study, the EPR model class in Eq. (21) was selected, since it resulted into both lower mean square error (MSE) and easily interpretable mathematical expressions.

$$G=a_0+\sum_{j=1}^{p} a_j.f((x_1)^{ES(j,1)}.....(x_k)^{ES(j,k)}) \qquad (21)$$

where *ES* is the matrix of exponents (coded as integers in the OPTIMOGA) and a_j parameter is estimated by using classical numerical regression methods like Least Squares or even Nonnegative Least Squares methods. It is worth to observe that *ES* may have values within a user-defined set of exponents including zero. The latter value permits deselecting one or more variables in some terms of the final expressions, resulting in parsimonious (less complex) mathematical expressions.

The Coefficient of Determination (CD), calculated as Eq. (22), is the criteria implemented to estimate the accuracy of the model. G_{Exp} and G_{Pred} are the actual (i.e. measured) target values and the output values of EPR models, respectively, and *N* is the number of training samples. Another setting of EPR for the present analysis is presented in Table 1. Suitable values for the range of exponents was achieved by trial and error [34]. 80% of all pattern data was considered to train process and the other 20% of the data was used in a test stage (i.e. as data was unseen during model development).

$$CD=1-\sum_{N}(G_{Pred}-G_{Exp})^2 / \sum_{N}(G_{Exp}-avg(G_{Exp}))^2 \qquad (22)$$

The EPR models are also evaluated in terms of their complexity (i.e. number of selected variables and/or number of terms) and only the models, which are the best compromising solutions among such objectives, are considered.

The analysis reported here has been performed using the EPR-MOGA-XL tool, version 1.0. EPR-MOGA-XL can be run as a function in MS-Excel as it is a smart add-in.

4. Results and discussion

The characteristics of the influent and effluent throughout the experiment in the UP/ASFF are shown in Table 2. Independent factors, influent COD, OLR, and HRT have been altered randomly.

4.1. Process analysis and effect of Food to Microorganism ratio (F/M)

F/M ratio is one of the most important biological parameters and a significant variation in this factor can cause serious problems in the process performance [48]. In general, the biological COD removal efficiency decreases by either working at the shorter HRT or higher F/M ratios due to the associated requiring time for COD consumption by microorganisms. Fig. 1 shows the average of the COD removal efficiency for each run along with various F/M ratios. COD removal efficiency and F/M ratio were in the range of 68- 95% and 0.50- 0.86 1/d, respectively. A sudden increase of OLR under maximum F/M ratio condition in run 8 resulted in high concentration of attached biomass and consequently clogging phenomenon through the column. As a result, COD removal performance was declined to 68%. This can be happened because of the problem in oxygen delivery deficiency at higher OLRs. Organic loading shock caused bulking phenomenon at the beginning of run 8, however, the performance of the system recovered rapidly. The color of the biomass was different at various OLRs and zones, in the bioreactor; the light yellow color biomass was predominant in the aerobic zone while dark brown color of the biomass in semi-anaerobic zone was in progress.

4.2. First-order kinetic model

At the steady state condition, the first-order COD removal relation was applied for biofilm reactor performance prediction. The value of K_1 was obtained from the slope of the line by plotting (S_i-S_e)/HRT versus S_e in Eq. (2). Fig. 2A shows the slope (K_1) and coefficient of determination of plot are 8.08 (1/d) and 0.45, respectively. The low value of R^2, clearly indicated that first-order kinetics cannot be proper for the prediction of effluent COD.

4.3. Grau second-order kinetic model

In order to determine the second-order kinetic coefficients (m, n and K_2) Eq. (5) was plotted in Fig. 2B. The values of m and n were calculated from the intercept and slope of the straight line on the graph. The constant values of m and n were found to be 0.03 and 1.03, respectively for synthetic municipal wastewater with a high coefficient of determination (R^2=0.99). The second-order removal rate constant (K_2) calculated from $m = S_i/ (K_2X)$ equation was found to be 10.2 (1/d), which depends on microorganism and influent COD concentration. The formulas to predict effluent COD concentrations were given in Eqs. (23-24) obtained by rearranging the Eq. (5) and substituting the values of m and n from Fig. 2B.

$$S_e = S_i (1-(\mathrm{HRT}/(m+n.\mathrm{HRT}))) \quad (23)$$

$$S_e = S_i (1-\mathrm{HRT}/(0.03+(1.03.\mathrm{HRT}))) \quad (24)$$

4.4. Modified Stover–Kincannon model

The results of the modified Stover-Kincannon model were shown in Fig. 2C. Under a steady state condition, the modified Stover-Kincannon model was applied to calculate COD degradation kinetics of the UP/ASFF system. Plotting $V/(Q(S_i-S_e))$ versus $V/(QS_i)$,

K_B/U_{max} and $1/U_{max}$ are the slope and intercept point, respectively. Accordingly, U_{max} and K_B constants were found to be 6.42 kg/(m^3.d) and 7.35 kg/(m^3.d), respectively. This indicates that maximum allowable COD removal rate in the biofilm bioreactor was calculated 6.42 kg/(m^3.d) while its actual value was obtained 3.25 kg/(m^3.d) (51% of the calculated U_{max}). The coefficient of determination of 0.99 was confirmed the applicability of the modified Stover-Kincannon model for COD removal prediction in the UP/ASFF system. After obtaining modified Stover-Kincannon models' constants, the effluent COD concentrations could be predicted by Eq. (25). Likewise, based on the modified Stover-Kincannon, COD removal efficiency can be predicated by Eq. (26).

$$S_e = S_i - 7.35 S_i / 6.42 + (Q.S_i / V) \quad (25)$$

$$E = 7.35/6.42 + (S_i/\mathrm{HRT}) \quad (26)$$

4.5. Monod and Contois models

In order to determine the kinetic coefficients of Monod model (Y, K_d, K_s, μ_{max}) from Eqs. (16-17), the VSS was measured for each run. The values of Y and K_d were determined by plotting $(S_i-S_e)/\mathrm{HRT}.X$ versus 1/SRT in Eq. (16), as demonstrated in Fig. 3A. The values for K_d and Y were found to be 0.30 (1/d) and 0.69 gVSS/(gCOD), respectively with the coefficient of determination of 0.85. By plotting $1/S_e$ versus $\mathrm{SRT}/(1+\mathrm{SRT}.K_d)$, the values of the maximum specific growth rate (μ_{max}) and half-velocity constant (K_s) for the Monod model could be obtained from Fig. 3B as 0.41 (1/d) and 3.57 (mg/L), respectively. Likewise, the similar procedure was employed for determination of Contois model kinetic constants.

$$q_{s,max} = \mu_{max} / Y \quad (27)$$

$$S_e = (1+0.30\mathrm{SRT})/(0.03\mathrm{SRT}-0.28) \quad (28)$$

$S_e = X.(1+0.30SRT)/(82SRT-703)$ (29)

The relationship between the SRT/(1+ SRT.K_d) and X/S_e was plotted in Fig. 3C and the values for β and μ_{max} were found to be 0.0014 (mgCOD/mgVSS) and 0.42 (1/d), respectively. Based on Eq. (27) the maximum specific substrate utilization rate ($q_{s,max}$) in this model could be achieved by dividing μ_{max} to Y as 0.60 gCOD/(gVSS.d) [49]. After defining the parameters of the model, effluent COD concentration is predictable by Eqs. (28-29). It is worth mentioning that the main disadvantage of Monod and Contois models is the limited prediction domain. For instance, in this work, the outcome results for the SRT under 10 days were not reliable to predict the performances of the process.

4.6. Hybrid modelling

To develop a model that accurately predicts the COD removal percentage, several attempts were made to simulate the process using the EPR-MOGA-XL software. The outcome of the EPR procedure is presented in Eqs. (30-34).

$E=85.63$ $CD_{train}=0.0$ $CD_{test}=0.0$ (30)

$E=66.8/OLR^{0.5}+38.75$ $CD_{train}=90.8$ $CD_{test}=89.4$ (31)

$E=(0.002859S_{in}/OLR)+(64.463/OLR^{0.5})+39.588$ $CD_{train}=91.0$ $CD_{test}=89.9$ (32)

$E=(53.884/OLR^{0.5})+(3.245S_{in}^{0.25}/OLR^{0.5})+(8488OLR^{0.5}/S_{in}^{1.5})+35.481$ $CD_{train}=91.8$ $CD_{test}=90.4$ (33)

$E=(26.7/t^{1.5}OLR^{1.5}S_{in}^{0.5})+(53.7/OLR^{0.5})+(3.25S_{in}^{0.25}/OLR^{0.5})+(8458OLR^{0.5}/S_{in}^{1.5})+35.54$ $CD_{train}=91.8$ $CD_{test}=89.8$ (34)

The models are sorted based on CD of training and level of complexity (i.e. number of terms and number of inputs in this case). EPR represents a set of multidimensional strategies for the selection of models, based on a comprehensive analysis of complexity

and prediction accuracy of the models. EPR can work either in single or multi-objective configurations. In single-objective EPR, an objective function is used to control the prediction accuracy of the models without permitting excessive complexities to enter the models. In the case of multi-objective strategy two or three objective functions are represented in which one of them will control the prediction accuracy of the models, while at least one objective function controls the complexity of the models. The multi-objective strategy returns a trade-off surface (or line) of complexity versus prediction accuracy which permits the user to compare models' expressions with each other, and then choose an appropriate model for the particular phenomenon. In this research, the EPR-MOGA-XL was used to develop the COD removal model. The first meaningful equation generated by EPR (i.e. Eq. 31) has a relatively high value of coefficient of determination for both training and testing (i.e. CD_{train}=90.8 and CD_{test} =89.4) and low complexity of mathematical structure. This equation contains only one of the input parameters (i.e. OLR) which implies the predominant effect of OLR on the removal efficiency. The inverse relationship between the OLR and *E* refers to the ratio of OLR to DO. At the constant HRT and DO, increasing the influent COD provides an inhibitory medium for microorganism activity, and then, disturbs the biofilm performance. This inverse relationship is explained through a limitation in oxygen mass transfer rate at the aerobic unit of bioreactor. To achieve higher removal efficiency and the effluent with lower effluent COD, the DO concentration must be maintained at the optimum level, particularly, where both semi-anaerobic and aerobic zones are connected without physical separation. In order to maintain oxygen consumption through microbial film, oxygen has to cross the biofilm-liquid interface and transfer through the biofilm. Since this mechanism of transferring is generally achieved by diffusion, a concentration gradient within biofilm is expected. Therefore, for various

DO values of bulk liquid, the penetration depth of oxygen is different [50]. Moreover, the overall amount of biomass attached to the carrier material increased as the OLR increases which results in channelization phenomenon in the bioreactor. Furthermore, because of the high influent load and high sludge production during the operating period, physical clogging of the system occurs leading to poor COD removal. Backwashing is the remedy of this insufficiency; however, it reduces the amount of active biomass in the bioreactor, which could potentially result in unstable bioreactor performance and increasing shear stress in the bioreactor. Addition of another term in Eq. (32) shows a non-significant enhancement of CD, although it shows the direct effect of influent COD on removal efficiency. Such a direct relationship is confirmed for the remaining models, although the increase of relevant complexity is not justified by an increase of model accuracy.

With regard to the proposed models by EPR, no meaningful effect of t (time) on the effluent COD confirms the validity of the assumption ($dS/dt = 0$) applied for the mechanistic approach. In addition, under a steady state condition, overall biofilm thickness and active biomass concentrations will reach a constant value; however, the biofilm attachment and detachment on support media occur dynamically.

Fluctuation of the COD removal percentage throughout the experiment is based on variations in two main factors of the influent COD and HRT, which is depicted in Fig. 4A. As shown in Fig. 4A (regarding Table. 2 for more understanding of the experimental strategy) a little more efficiency of the bioreactor performance at run 7 rather than run 4 at similar OLR of 2 kg/(m^3.d), could be related to their variations in HRT. The higher liquid velocity in the bioreactor provides an improvement in the mass transfer rate, and consequently, the faster COD removal rate. However, high flow velocity means a high shear stress at the biofilm surface, which generates a greater

detachment rate. Among the proposed models by EPR, Eq. (31) with minimum number of terms and input variables was selected to illustrate Fig. 4B. In Fig. 4B experimental and predicted COD removals were compared satisfactorily with R^2 of 0.91 according to Eq. (31).

4.7. Evaluation of models

Table 3 summarizes the part of the substrate removal kinetic constants with the corresponding OLR that have been compared with the results obtained from other researches [51,52,53,54], however, the rest of the kinetic constants are illustrated in Table 4. The calculated microbial death rate constant (0.30 1/d) was higher than the value obtained by Pirsaheb *et al* that used phthalic acid (0.11 1/d) and dimethyl phthalate (0.06 1/d) as substrates [55]. Furthermore, the lower ratio of K_s to the influent COD points toward the high affinity of microorganism to the substrate. The juxtaposition of the kinetic constants for Contois, first-order (K_1), and second-order (K_2) revealed that maximum substrate utilization rate ($q_{s,max}$) for Contois model was lower than other values. Generally, the differences among the kinetic constants can be essentially attributed to the type of substrate, reactor configurations, range of applied OLR, and differences in other operating conditions such as temperature.

With respect to the statistical analysis and other calculated criteria for models shown in Table 5, it seems that the hybrid approach had a considerable robustness in the modelling performance. While from mechanistic approaches, modified Stover–Kincannon kinetic was recognized more appropriate for COD removal prediction than the rest of the models.

To test the validity and capability of the models, results obtained from the experimental data for effluent COD were compared with the predicted values. Apart from low R^2

value, the serious problem of Monod equation is related to its inability to predict all ranges of influent, in particular in some experimental runs, which were done at SRT under 9 days. As applied OLR of 4.8 is out of range, Monod equation is not proper for prediction in this case. There is a similar problem for Contois model as these two equations (Eqs. (28 and 29)) have the same form of relation in denominator. However, a coefficient of X can act as a balancer in Contois prediction process so that 8 out of 9 experimental runs were used in this study. Although the Contois model shows acceptable coefficient of determination for prediction of effluent COD, it was not the same as the modified Stover-Kincannon. In addition to an unsatisfactory correlation among the outputs in first-order model, the high value of normalized MSE apparently showed that there should be a meaningful difference between predicted and experimental values. Among the models, second-order predictor was the sole model that the statistical F-test analysis showed the unequal variances between experimental values and calculated data through the Eq. (24). Whereas, from the statistical analysis among the mechanistic models, modified Stover-Kincannon showed a high degree of reliability in terms of the lowest normalized MSE (0.02) and the highest R^2 (0.92).

On the other hand, the semi-mechanistic technique does not bear enumerated disadvantages associated with mechanistic models, and also, statistically, it was more accurate. Considering a process in a steady state condition is the main specification of modified Stover-Kincannon, as there is no such assumption in EPR, and this is the main superiority of EPR over mechanistic models. As shown in Table 5, the EPR model shows a very good value of the R^2 and other statistical values. Despite the flexibility of this approach, it represents a group of explicit expressions with different accuracy and the degree of complexity of mathematical structures. Therefore, it could be a rewarding approach where a prediction of a complex process like multiphase biofilm reactor is

desirable. Moreover, EPR approach with providing insights into the process (in what way the model's inputs affect outputs) showed that it could be the best option for the prediction of UP/ASFF performance, even though mechanistic approaches such as modified Stover-Kincannon are also desirable.

5. Conclusion

Sustainability at higher OLR, effluent with high quality, and less waste production are some of the advantages of the UP/ASFF system over other biofilm bioreactors comprising single compartment of anaerobic or aerobic. Two paths of mechanistic and hybrid approaches were investigated to model the performance of UP/ASFF systems. The mechanistic path was conducted by kinetics study, including Monod, Contois, Grau second-order, modified Stover-Kincannon, and first-order. In addition, a novel state of the art modelling technique based on evolutionary computing EPR was employed to develop an accurate explicit model. This new methodology is based on both numerical and symbolic regressions. Model validation and statistical analysis confirmed that the output data predicted by EPR had the most adjacency to the experimental results with a coefficient of determination of 0.93, and the lowest normalized MSE of 0.02. The present study demonstrates that the EPR model has some potentials to be used for the design of full-scale UP/ASFFs to treat municipal wastewater.

References

[1] S. Karthikeyan, V. Gupta, R. Boopathy, A. Titus, G. Sekaran, J. Mol. Liq. 173 (2012) 153-163.

[2] T.A. Saleh, V.K. Gupta, Sep. Purif. Technol 89 (2012) 245-251.

[3] R. Saravanan, S. Karthikeyan, V. Gupta, G. Sekaran, V. Narayanan, A. Stephen, Mater Sci Eng C 33 (2013) 91-98.

[4] A. Mittal, J. Mittal, A. Malviya, V. Gupta, J. Colloid Interface Sci. 344 (2010) 497-507.

[5] V.K. Gupta, R. Jain, A. Nayak, S. Agarwal, M. Shrivastava, Mater. Sci. Eng. C 31 (2011) 1062-1067.

[6] T.A. Saleh, V.K. Gupta, Adv. Colloid Interface Sci. 211 (2014) 93-101.

[7] V.K. Gupta, R. Kumar, A. Nayak, T.A. Saleh, M. Barakat, Adv. Colloid Interface Sci. 193 (2013) 24-34.

[8] R. Saravanan, V. Gupta, E. Mosquera, F. Gracia, J. Mol. Liq. 198 (2014) 409-412.

[9] A. Mittal, D. Kaur, A. Malviya, J. Mittal, V. Gupta, J. Colloid Interface Sci. 337 (2009) 345-354.

[10] A. Mittal, J. Mittal, A. Malviya, V. Gupta, J. Colloid Interface Sci. 340 (2009) 16-26.

[11] A. Mittal, J. Mittal, A. Malviya, D. Kaur, V. Gupta, J. Colloid Interface Sci. 342 (2010) 518-527.

[12] V.K. Gupta, A. Mittal, D. Jhare, J. Mittal, RSC adv 2 (2012) 8381-8389.

[13] M. Ahmaruzzaman, V.K. Gupta, J. Ind. Eng. Chem. 50 (2011) 13589-13613.

[14] T.A. Saleh, V.K. Gupta, Environ. Sci. Pollut. Res. 19 (2012) 1224-1228.

[15] R. Saravanan, V. Gupta, V. Narayanan, A. Stephen, J. Taiwan Inst. Chem. Eng. 45 (2014) 1910-1917.

[16] V. Gupta, A. Nayak, Chem. Eng. J. 180 (2012) 81-90.

[17] B. Khorshidi, A. Bhinder, T. Thundat, D. Pernitsky, M. Sadrzadeh, J. Membr. Sci. 511 (2016) 29-39.

[18] H. Wu, G. Zeng, J. Liang, J. Chen, J. Xu, J. Dai, X. Li, M. Chen, P. Xu, Y. Zhou, Appl. Microbiol. Biotechnol. 100 (2016) 8583-8591.

[19] G. Zeng, H. Wu, J. Liang, S. Guo, L. Huang, P. Xu, Y. Liu, Y. Yuan, X. He, Y. He, RSC Adv. 5 (2015) 34541-34548.

[20] H. Wu, C. Lai, G. Zeng, J. Liang, J. Chen, J. Xu, J. Dai, X. Li, J. Liu, M. Chen, Crit. Rev. Biotechnol. 37 (2017) 754-764.

[21] F. Tazari, M. Rahaie, A.H. Zarmi, H. Jalili, F. Yazdian, S.A. Kordkandi, Bioprocess Engineering 1 (2017) 14-20.

[22] H. Horn, S. Lackner, Springer, 2014, pp. 53-76.

[23] S.A. Kordkandi, A.B. Khoshfetrat, J. Ind. Eng. Chem. 31 (2015) 257-262.

[24] M. Forouzesh, A.B. Khoshfetrat, S.A. Kordkandi, Water Sci. Technol. 76 (2017) 877-884.

[25] S.A. Kordkandi, L. Berardi, Biochem. Eng. J. 103 (2015) 170-176.

[26] M. Jelali, A. Kroll, Springer London, 2003.

[27] A. Mittal, D. Kaur, A. Malviya, J. Mittal, V. Gupta, J. Colloid Interface Sci. 337 (2009) 345-354.

[28] A. Mittal, J. Mittal, A. Malviya, V. Gupta, J. Colloid Interface Sci. 340 (2009) 16-26.

[29] V.K. Gupta, R. Jain, A. Nayak, S. Agarwal, M. Shrivastava, Mater. Sci. Eng. C 31 (2011) 1062-1067.

[30] S. Karthikeyan, V. Gupta, R. Boopathy, A. Titus, G. Sekaran, J. Mol. Liq. 173 (2012) 153-163.

[31] R. Saravanan, E. Sacari, F. Gracia, M.M. Khan, E. Mosquera, V.K. Gupta, J. Mol. Liq. 221 (2016) 1029-1033.

[32] E. Padilla-Gasca, A.L. López, J. Bioremed. Biodegrad. 1 (2010) 106-112.

[33] S. Han, Q. Yue, M. Yue, B. Gao, Y. Zhao, W. Cheng, Bioresour. Technol. 100 (2009) 1149-1155.

[34] K. Yetilmezsoy, Bioresour. Technol. 118 (2012) 89–101.

[35] F.R. Fia, A.T. Matos, A.C. Borges, R. Fia, P.R. Cecon, J. Environ. Manage. 108 (2012) 14-21.

[36] L. Sun, S. Wan, Z. Yu, Y. Wang, S. Wang, Bioresour. Technol. 104 (2012) 280-288.

[37] R. Rajagopal, M. Torrijos, P. Kumar, I. Mehrotra, J. Environ. Manage. 116 (2013) 101-106.

[38] A.M. Alani, A. Faramarzi, M. Mahmoodian, K.F. Tee, Environ. Technol. 35 (2014) 1721-1728.

[39] A. Faramarzi, A.A. Javadi, A. Ahangar-Asr, Comput. Struct. 118 (2013) 100-108.

[40] O. Giustolisi, D. Savic, J. Hydroinf. 8 (2006) 207-222.

[41] A. Nassr, A. Javadi, A. Faramarzi, Int. J. Numer. Anal. Meth. Geomech. (2017) DOI: 10.1002/nag.2747.

[42] S. Borghei, M. Sharbatmaleki, P. Pourrezaie, G. Borghei, Bioresour. Technol. 99 (2008) 1118-1124.

[43] A.D. Eaton, M.A.H. Franson, A.P.H. Association, A.W.W. Association, W.E. Federation, 2005.

[44] Q.A. Acton, 2011 Edition, Scholarly Editions, 2012.

[45] P. Grau, M. Dohanyos, J. Chudoba, Water Res. 9 (1975) 637-642.

[46] W.E. Federation, Biofilm Reactors WEF MOP 35, McGraw-Hill Education, 2010.

[47] S.-Q. Ni, S. Sung, Q.-Y. Yue, B.-Y. Gao, Ecol. Eng. 38 (2012) 30-36.

[48] R.T. Alqahtani, M.I. Nelson, A.L. Worthy, Chem. Eng. J. 218 (2013) 99-107.

[49] O. Giustolisi, D. Savic, J. Hydroinf. 11 (2009) 225-236.

[50] D. Laucelli, O. Giustolisi, Environ. Modell. Software 26 (2011) 498-509.

[51] L. Berardi, Z. Kapelan, O. Giustolisi, D. Savic, J. Hydroinf. 10 (2008) 113-126.

[52] E. Amanatidou, G. Samiotis, D. Bellos, G. Pekridis, E. Trikoilidou, Bioresour. Technol. 182 (2015) 193-199.

[53] D. Herbert, R. Elsworth, R. Telling, J. Gen. Microbiol. 14 (1956) 601-622.

[54] C. Nicolella, M. Van Loosdrecht, J. Heijnen, J. Biotechnol. 80 (2000) 1-33.

[55] A. Noroozi, M. Farhadian, A. Solaimanynazar, Desalin. Water Treat. (2014) 1-8.

[56] A.H. Moghaddam, J. Sargolzaei, J. Taiwan Inst. Chem. Eng. 49 (2014) 165–171.

[57] M.K. Sharma, A.A. Kazmi, Sep. Sci. Technol. 50 (2015) 2752-2758.

[58] A. Akhbari, A. Zinatizadeh, P. Mohammadi, Y. Mansouri, M. Irandoust, M. Isa, Int. J. Environ. Sci. Technol. 9 (2012) 371-378.

[59] M. Pirsaheb, A.-R. Mesdaghinia, S.J. Shahtaheri, A.A. Zinatizadeh, J. Hazard. Mater. 167 (2009) 500-506

List of figures:

Fig. 1. F/M ratios and COD removal efficiencies for runs carried out in experiments.

Fig. 2. First-order (A), Second-order (B), and the Modified Stover–Kincannon kinetic model plots (C).

Fig. 3. Determination of Y, K_d (A), μ_{max}, and K_S (B) for Monod kinetic constants along with μ_{max} and β for Contois kinetic constants (C).

Fig. 4. Measured and calculated COD removal throughout the experiments (A) and comparisons based on Equation (31) (B).

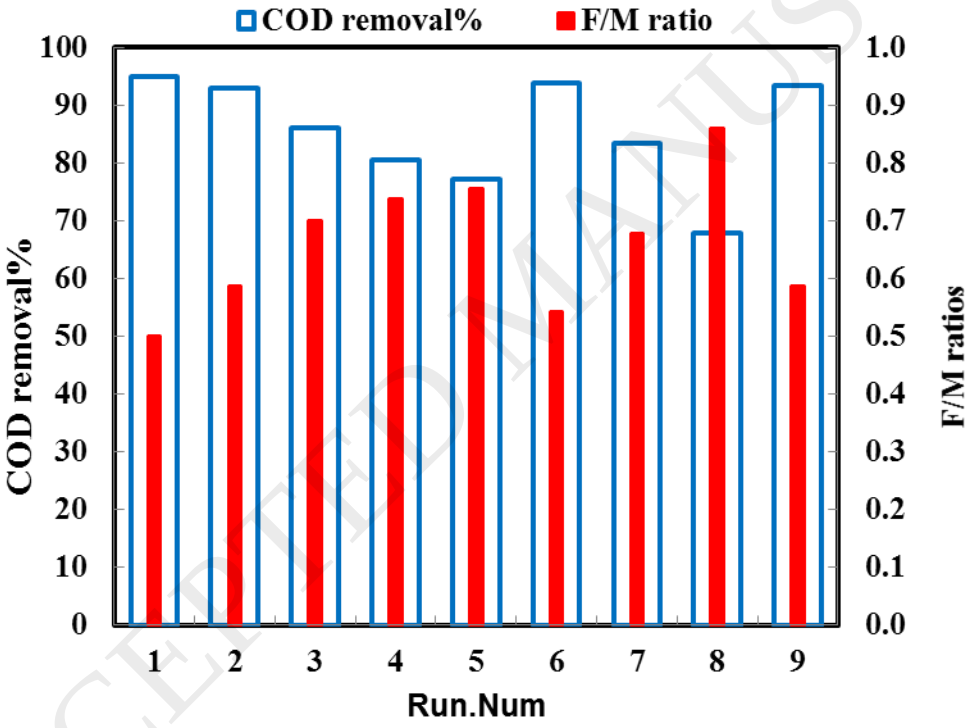

Fig. 1

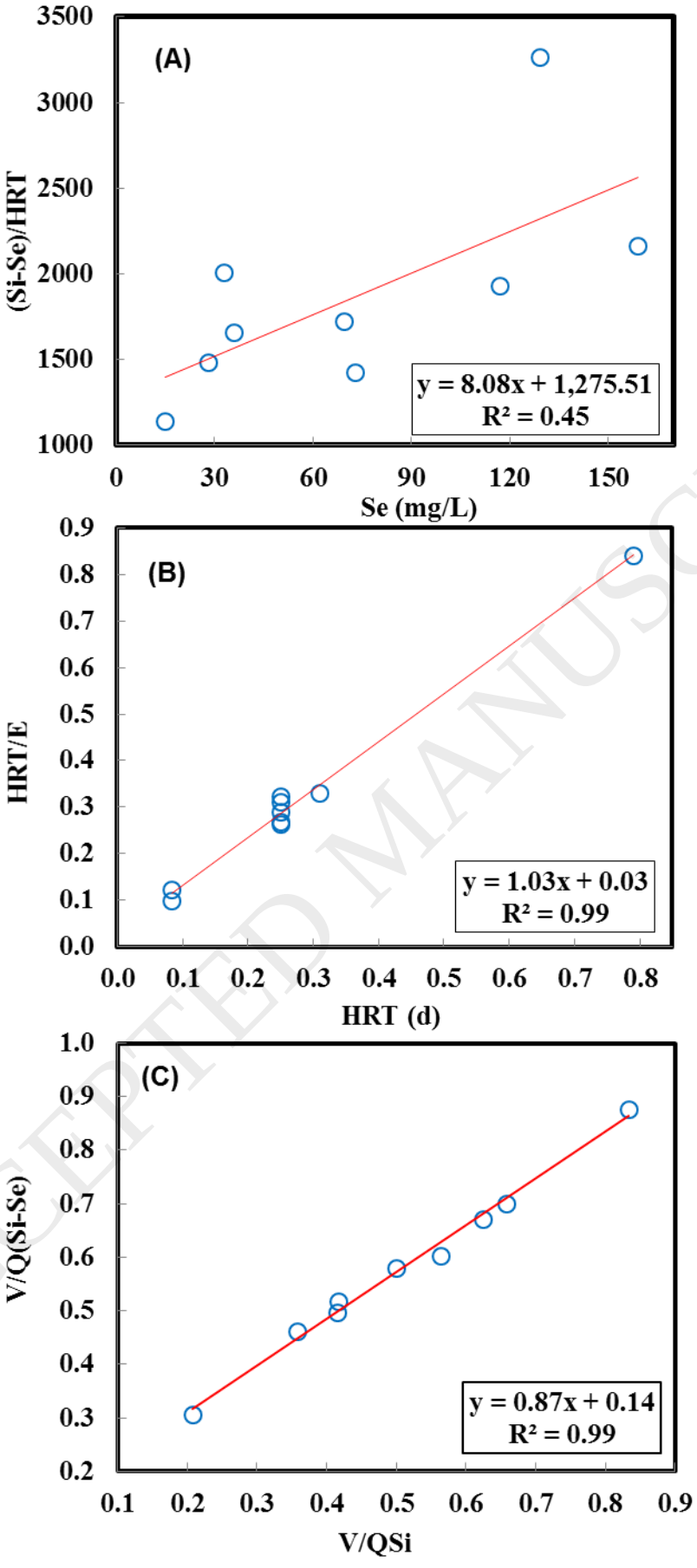

Fig. 2

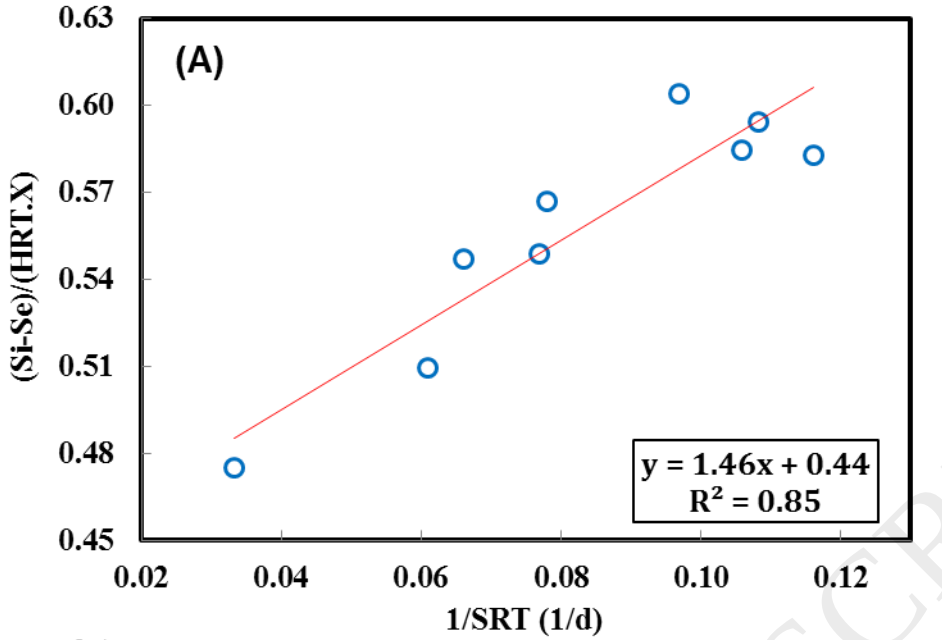

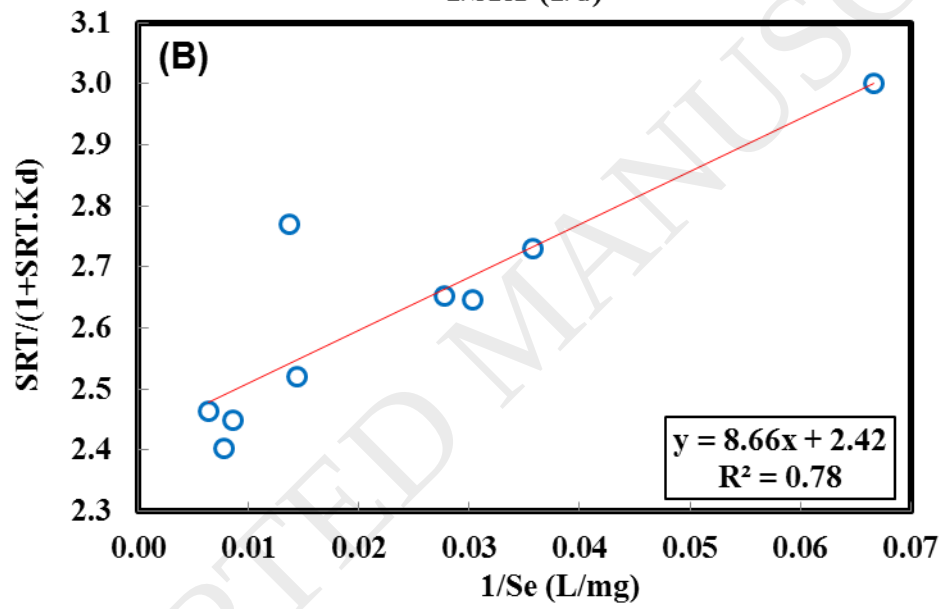

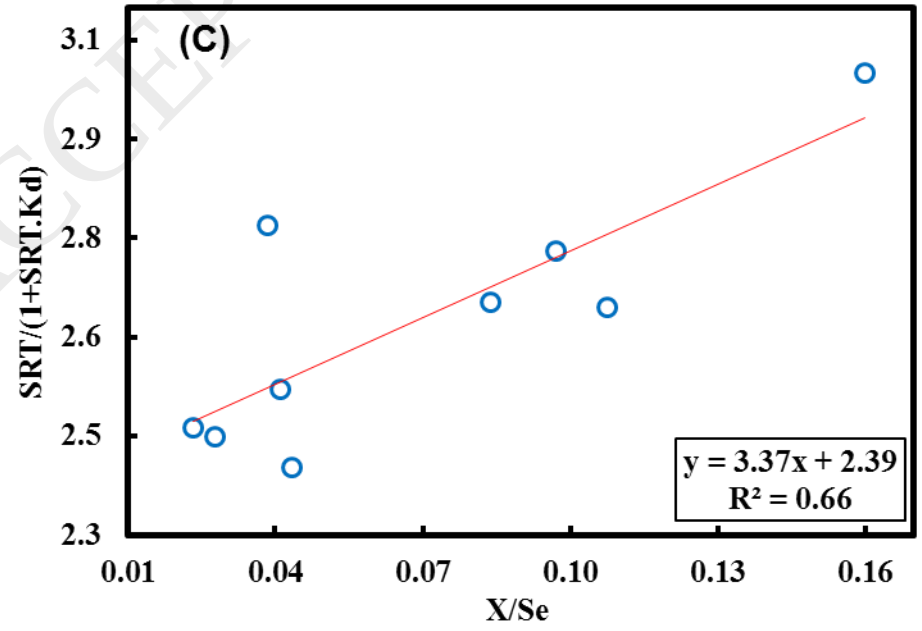

Fig. 3

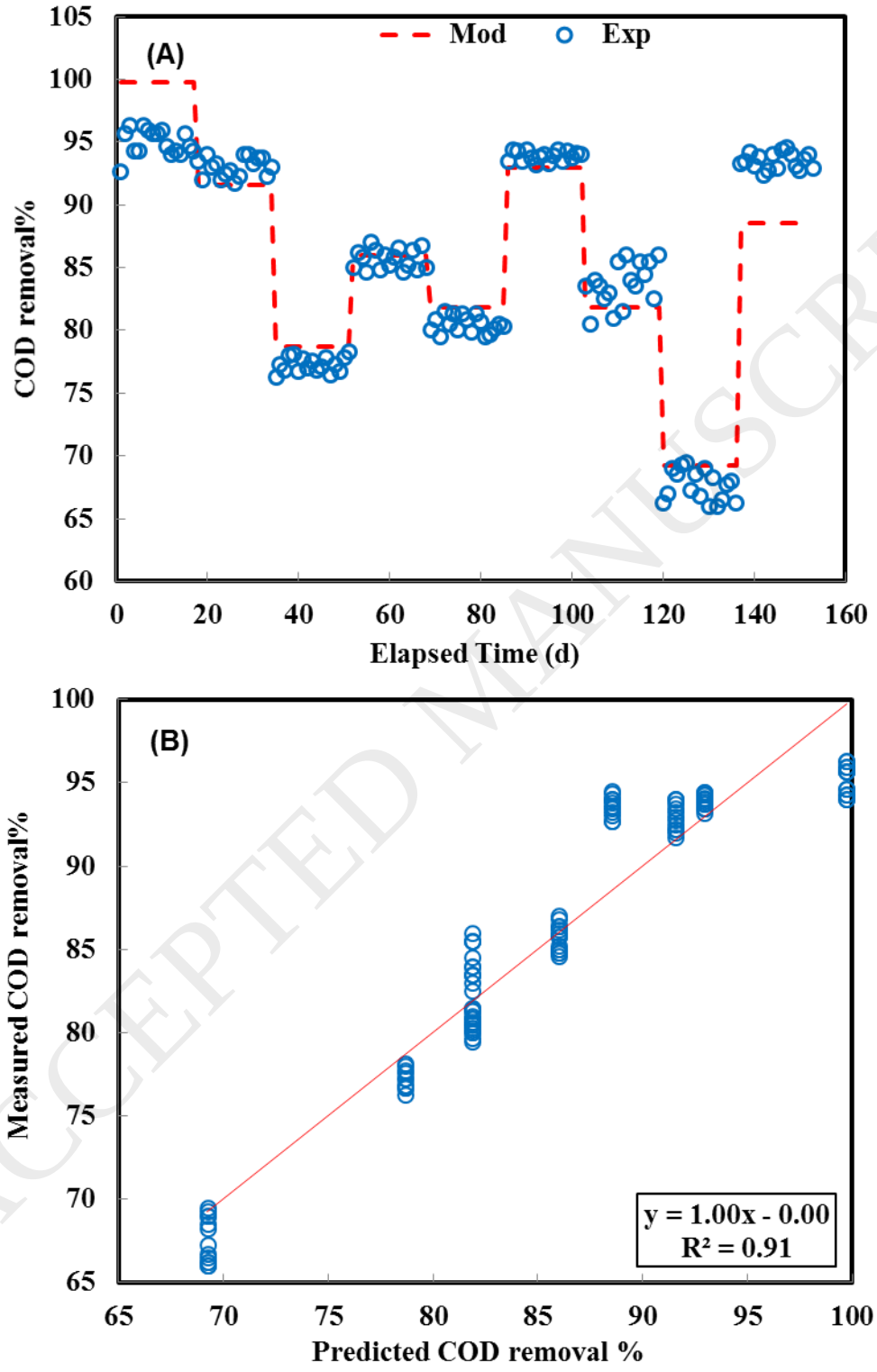

Fig. 4

List of Tables:

Table 1. Setting of parameters for EPR.

EPR type	Regression type	Function	Range of exponents	Numerical Regression
Case 2	Static	No function	[-3:0.5: 3]	Non-negative Least Squares

Table 2. Average experimental data obtained under steady-state conditions.

Run	Influent COD (mg/L)	HRT(d)	OLR (kg/(m^3.d))	Effluent COD (mg/L)	OLR removal (kg/(m^3.d))	pH
1	300	0.25	1.2	15	1.14	7.3
2	400	0.25	1.6	28	1.49	7.41
3	700	0.25	2.8	159	1.72	7.54
4	500	0.25	2	70	1.93	7.6
5	600	0.25	2.4	117	2.16	7.66
6	1200	0.79	1.5	73	1.43	7.64
7	200	0.08	2.4	33	2.01	7.48
8	400	0.08	4.8	129	3.27	7.85
9	550	0.3	1.8	36	1.66	8

Table 3. Comparison of Modified Stover–Kincannon and Second order kinetic parameters for various studies.

wastewater Type	OLR	Modified Stover–Kincannon		Second order			Reference
		U_{max}	K_B	K_2	m	n	
Municipal	0.8-2	57.5	62.6	8.24	0.005	1.11	[36]
Synthetic	5.4-12	6.5	9.2	-	0.02	1.4	[37]
Synthetic	1.7-2.9	15.2	14.8	-	-	-	[38]
Domestic	1.3-5.9	0.74	0.93	0.26	0.22	1.09	[39]
Synthetic	1.2-4.8	6.42	7.35	10.2	0.03	1.03	This study

Table 3. Summarized kinetic parameters for Monod, Contois and first-order models.

Kinetic models	Kinetic parameters	Values
Monod	μ_{max}	0.41
	K_d	0.30
	Y	0.68
	K_S	3.58
Contois	β	1.41
	$q_{s,max}$	0.60
	μ_{max}	0.42
First-order	K_1	8.079

Table 5. Comparison of both hybrid and mechanistic models' performance based on statistical analysis.

Models	Types of model	P-value	F-test	F-Critical	Degree of freedom	Normalized MSE	R^2
First order	Mechanistic	0.88	1.12	3.44	8	1.00	0.59
Second order	Mechanistic	0.03	5.53	3.44	8	0.11	0.41
Modified Stover Kincannon	Mechanistic	0.80	1.20	3.44	8	0.02	0.92
Monod	Mechanistic	0.30	0.44	0.26	7	0.18	0.72
Contois	Mechanistic	0.27	0.42	0.26	7	0.17	0.78
EPR	Semi-Mechanistic	0.84	1.16	3.44	8	0.02	0.93